Late Caledonian transpression and the structural controls on pluton construction; new insights from the Omey Pluton, western Ireland.
William McCarthy, R. John Reavy, Carl T. Stevenson & Michael S. Petronis
Earth and Environmental Science Transactions of the Royal Society of Edinburgh **106** (2015), 11–28

Appendix - Supplementary Magnetic Data

Investigation of rock magnetic properties for AMS interpretation

Measurement of AMS produces a second-rank tensor, of which the orientation and magnitude of its principal axes ($K1 \geq K2 \geq K3$) are dependent on the degree of alignment of individual minerals in a sub-specimen and the inherent magnetic susceptibility of different mineral phases (Nagata 1961; Khan 1962). The size, shape, intensity and axes orientations can be typically linked to an observed petrofabric (e.g., Knight & Walker 1988; Archanjo *et al.* 1995; Launeau & Cruden 1998), although some caveats exist such as inverse magnetic fabrics (Potter & Stephenson 1988; Rochette 1988), textural anisotropy and magnetic interaction (Wolff *et al.* 1989; Gaillot *et al.* 2006), and mineralogical control over AMS (Rochette & Vialon 1984; Borradaile *et al.* 1987; Jackson 1991). These caveats are well documented and can be accounted for (Tarling & Hrouda 1993; Borradaile & Jackson 2010).

We used AMS to investigate the structural relationship between subtle fabrics associated with the emplacement of the Omey pluton and the obvious, but localised, NNW–SSE shear zones. We undertook a standardised suite of rock magnetic experiments to determine magnetic mineralogy, coercivity spectra and grain size (Lowrie & Fuller 1971; Bailey & Dunlop 1983; Dunlop 1986; Argyle & Dunlop 1990; Heider *et al.* 1992; Argyle *et al.* 1994; Xu & Dunlop 1995; Dunlop & Özdemir 1997). These data were used in conjunction with our field and petrographic observations and the statistical treatment of each AMS tensor (Owens 1974, 2000; Jelinek 1977, 1981) to determine the significance of each averaged AMS site. Our results are presented in Figure 1 and summarised in Table 1.

Table 1 Summary of compiled rock magnetic properties

		Coercivity		Demagnetization Characteristics				Susceptibility	Curie Temp. (°C)		
Sample	Facies	H_{CR} (A/m)	M_S (A/m)	MDF_{AR} M	MDF_{IR} M	MDF_{ARM}/IRM_{MDF}	Remanence Field	$K_{mean} \times 10^{-3}$	Heating	Cooling	Inferred grain size & domain state
OM42	G1	-0.031	0.4–0.3	5	8.5	0.59	Low Field	7.83	576	578	MD (~130μm)
OM70	G2	-0.055	0.4–0.5	13.5	17.5	0.77	Low Field	12.77	579	579	MD (~13μm)
OM73	G3	-0.068	0.5–0.7	17	20.5	0.83	Low Field	3.11	580	580	MD - PSD (~3μm)
OM95	G1	-0.048	0.4	9.5	21	0.45	Low Field	6.05	579	576	MD (~110μm)
OM106	G3	-0.063	0.4–0.5	14	23	0.61	Low Field	5.08	577	578	MD - PSD (~5μm)
OM108	G3	-0.046	0.4	9.5	18	0.53	Low Field	10.16	579	577	MD (110μm)

Figure 1 (A) Results of high temperature low field magnetic susceptibility experiments indicate magnetite is the most prominent ferromagnetic phase in all specimens. (B) Results of cryogenic low field magnetic susceptibility experiments show a negligible influence of paramagnetic phases at room temperature. (C & D) Results of IRM acquisition and back-field IRM demagnetisation show low coercivity behaviour characteristic of multi-domain–pseudo-single magnetite. (E) Response of select samples to demagnetisation of NRM, ARM and IRM show the median destructive field is always <21 mT, again indicating multi-domain magnetite is the principal contributor to remanence.

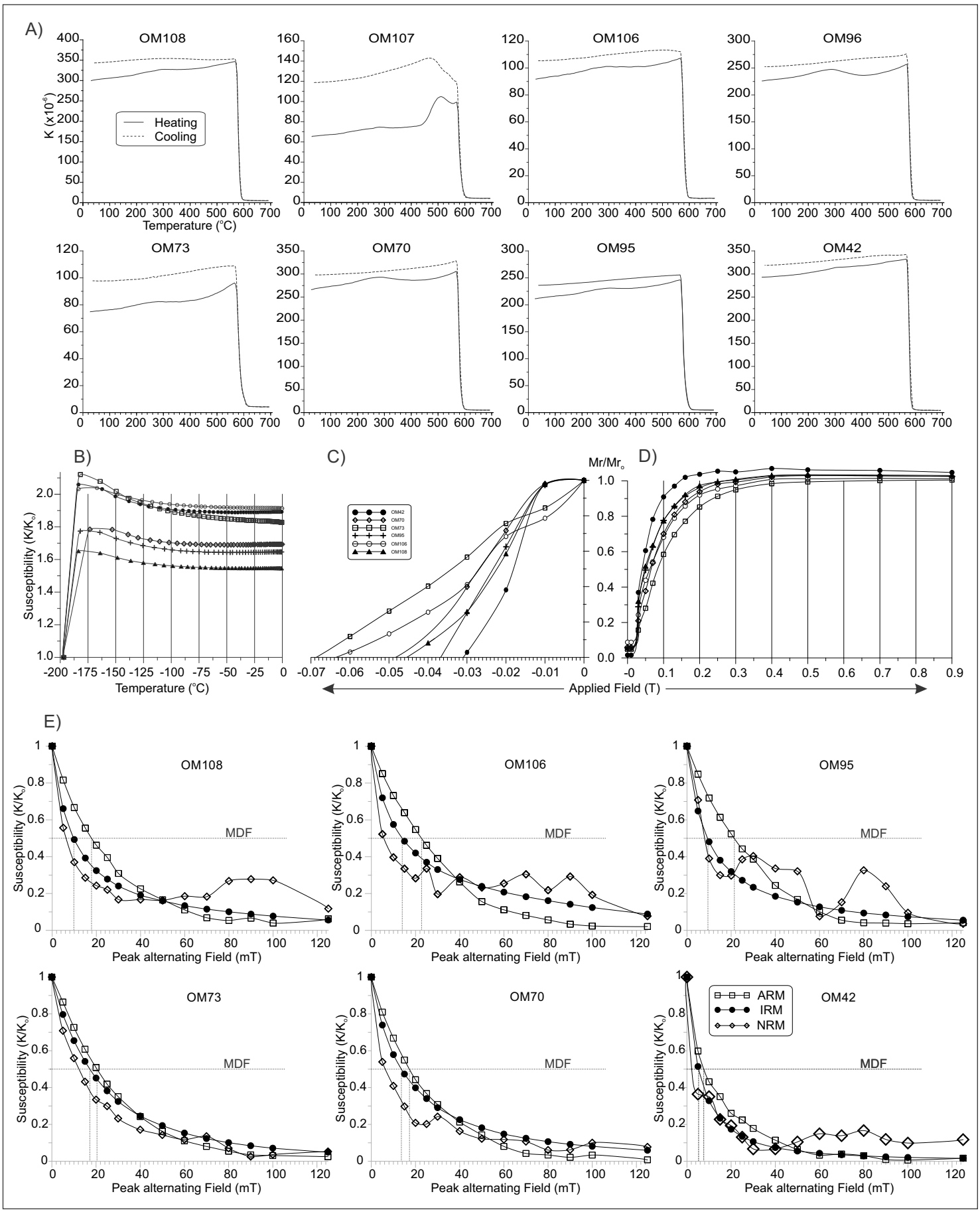
A)
OM108
OM107
OM106
OM96
OM73
OM70
OM95
OM42
K (x10⁻⁶)
Heating
Cooling
Temperature (°C)
B)
Susceptibility (K/K₀)
Temperature (°C)
C)
Mr/Mr₀
Applied Field (T)
D)
E)
MDF
Susceptibility (K/K₀)
Peak alternating Field (mT)
ARM
IRM
NRM

Temperature curves

The heating–cooling curves show that all samples behaved similarly and are essentially irreversible: susceptibility increased rapidly between minus 195°C and minus 174°C, followed by a moderate decline between minus 174°C and minus 125°C; whereas between minus 125°C and 12°C, no significant change occurred (Fig. 1a, b). These data are consistent with the presence of a ferromagnetic phase as the principal magnetic mineral in all sub-specimens, in this case biotite and minor amphibole, which caused the minor negative temperature dependence between minus 174°C and minus 125°C. Critically, the relative magnitude of susceptibility at room temperature, compared to that under cryogenic conditions, shows that the ferromagnetic component is the overwhelmingly dominant contributor to susceptibility, and therefore AMS, at room temperature.

A net increase in susceptibility is always observed after heating, and irreversible thermomagnetic curves such as these reflect the presence of either ferromagnetic iron sulphide phases, such as pyrrhotite, or the presence of coarse-grained maghemite; the latter is due to a low-temperature oxidisation process (initiated at <250°C) which converts Fe_2O_3 to Fe_3O_4 to form maghemite, which is metastable and inverts to magnetite above 300°C (Dunlop & Özdemir 1997). The subtle bumps on our heating curves are considered to be a product of this process rather than to significant volumes of sulphide minerals, as petrographic analysis (Feely *et al.* 2007) does not support the latter scenario.

Curie Point (T_C) estimates for selected sub-specimens were determined by continuous measurement of low field susceptibility during step-wise heating and cooling of powdered samples between 30°C and 700°C (Fig. 1a). Using either the Hopkinson Peak or the inflection point methods (Hopkinson 1890; Tauxe 1998), eight samples return an inferred T_C of between 575°C and 580°C; whereas the 9th (sample OM89) yields a T_C of 590°C. The majority exhibit broad Hopkinson Peaks and only minor increases in susceptibility immediately prior to T_C; we interpret this as being consistent with a multi- (MD) to pseudo-single (PSD) domain magnetite grain size (Dunlop & Özdemir 1997). Our results are also consistent with MD to PSD low Ti titanomagnetite as the dominant ferromagnetic phase (e.g., Akimoto 1962; Readman & O'Reilly 1972; Orlický 1990; Liss *et al.* 2004; Lattard *et al.* 2006). For these, T_C can be used to determine average Ti (Akimoto 1962); hence all our samples have calculated Ti content of $\leq$0.1 %.

Demagnetisation behaviour

Natural remanent magnetisation (NRM) demagnetisation curves for all samples exhibit an initial rapid decrease in median destructive field (MDF) remanence (MDF $\leq$10 mT), with minor subsequent undulations (Fig. 1e). Anhysteretic remanent magnetisation (ARM) and saturation isothermal remanent

magnetisation (SIRM) also demagnetise in an exponential fashion. A narrow spectrum of L-type demagnetisation behaviour (Xu & Dunlop 1995) exists in the current data set (Table 1). MDF_{ARM} and MDF_{SIRM} ratios fall between 0.4 and 0.9, and exponential demagnetisation of ARM occurs in relatively low fields (MDF ≤25 mT). Together, these data indicate that a PSD to MD magnetic grain size is the dominant ferromagnetic phase in all sub-specimens (Argyle & Dunlop 1990; Xu & Dunlop 1995).

IRM and BIRM acquisition

Acquisition of saturation isothermal remanent magnetisation (IRM) and back-field isothermal remanent magnetisation (BIRM) was used to determine hysteresis, coercivity parameters and magnetic mineralogy and grain size. IRM acquisition curves (Fig. 1d) show that all samples reach 95 % saturation between 0.12 T and 0.3 T, with complete saturation between 0.3 T and 0.7 T (Table 1). Above 0.7 T and up to 2.5 T, no significant increase in magnetic remanence is observed. These observations are supported by BIRM data, which show a rapid decline in magnetic remanence between 0.01 T and 0.03 T (Fig. 1c). Coercivity of remanence (H_{CR}) is achieved in fields between 0.03 mT and 0.68 mT (Table 1). Facies G3 sub-specimens exhibit higher H_{CR}, between -0.068 mT and -0.046 mT, compared to Facies G2/G1 samples of 0.055–0.03 T (Table 1). These results complement IRM acquisition curves which show that Facies G3 samples require greater inducing fields (0.4–0.68 T) in order to reach full saturation; in comparison to sub-specimens from facies G1 and G2 (0.3–0.5 T).

Rapid acquisition of saturation (95 %) IRM in fields of ≤ 0.3 T, and H_{CR} values of < 0.07 T are consistent with the above observations and imply that PSD–MD titanomagnetite is the primary ferromagnetic mineral in all sub-specimens. Continued acquisition of remanence (< 5 %) in fields above 0.3 T shows that small amounts of higher coercivity minerals are present, such as maghemite or hematite, particularly in Facies G3. This observation is consistent with petrographic observations (Townend 1966; Feely *et al.* 2007) which identify a higher abundance of haematite and hydrothermal molybdenite disseminated in facies G2 and G3.

Characterisation of magnetic mineralogy

High-temperature, low field magnetic susceptibility experiments consistently return a T_C of between 575°C and 580°C, and show that low Ti titanomagnetite is the most abundant ferromagnetic mineral in the studied samples. Exponential demagnetisation of magnetic remanence, and the characteristically low coercivity values detected during IRM experiments, indicate that PSD to MD titanomagnetite grains dominate (Dunlop & Özdemir 1997). Therefore, the AMS fabric is expected to be "normal" (Rochette *et al.* 1999; Ferré 2002). Titanomagnetite is several orders of magnitude more susceptible than paramagnetic

minerals at room temperature in low fields, and thus the AMS tensor is expected to reflect the crystallographic orientation of this mineral where <5 % paramagnetic minerals are present (Pierre & Rochette 1987; Archanjo *et al.* 1995). Some G3 samples return very low K_{mean} values; in these cases a more substantial contribution by paramagnetic phases to the AMS tensor is expected. However, cryogenic experiments show that the paramagnetic contribution to bulk susceptibility in weakly magnetic samples (K_{mean} ~10^{-6}) remains negligible at room temperature. The petrographic observation that elongate titanomagnetite occurs along cleavage planes of paramagnetic minerals, combined with rock magnetic data which show magnetic susceptibility to be titanomagnetite-dependant, demonstrates that the titanomagnetite petrofabric can itself be dictated by the orientation of silicate minerals (Archanjo *et al.* 1995; Launeau & Cruden 1998).

References

Akimoto, S. 1962. Magnetic properties of $FeO–Fe_2O_3–TiO_2$ system as a basis of rock magnetism. *Journal of Physics Society Japan* **17(**Suppl.), 706–10.

Archanjo, C. J., Launeau, P. & Bouchez, J. L. 1995. Magnetic fabric vs. magnetite and biotite shape fabrics of the magnetite-bearing granite pluton of Gameleiras (Northeast Brazil). *Physics of the Earth and Planetary Interiors* **89**(1–2), 63–75. Available at: http://www.sciencedirect.com/science/article/pii/003192019402997P.

Argyle, K. S., Dunlop, D. J. & Xu, S. 1994. Single-domain behavior of multi-domain magnetite grains (Abstract). *Eos (Transactions of the American Geopysical Union)* **75**(Fall meeting suppl.), 196.

Argyle, K. S. & Dunlop, D. J. 1990. Low-Temperature and High-Temperature Hysteresis of Small Multidomain Magnetites (215–540 nm). *Journal of Geophysical Research* **95**(B5), 7069–82. Available at: http://dx.doi.org/10.1029/JB095iB05p07069.

Bailey, M. E. & Dunlop, D. J. 1983. Alternating field characteristics of pseudo-single-domain (2–14 μm) and multidomain magnetite. *Earth and Planetary Science Letters* **63**(3), 335–52.

Borradaile, G., Keeler, W., Alford, C. & Sarvas, P. 1987. Anisotropy of magnetic susceptibility of some metamorphic minerals. *Physics of the Earth and Planetary Interiors* **48**(1–2), 161–66. Available at: http://www.sciencedirect.com/science/article/pii/0031920187901191.

Borradaile, G. J. & Jackson, M. 2010. Structural geology, petrofabrics and magnetic fabrics (AMS, AARM, AIRM). *Journal of Structural Geology* **32**(10), 1519–51. Available at: http://linkinghub.elsevier.com/retrieve/pii/S0191814109002041.

Dunlop, D. J. 1986. Hysteresis Properties of Magnetite and their Dependence on Particle Size: A Test of Pseudo-Single-Domain Remanence Models. *Journal of Geophysical Research* **91**(B9), 9569–84. Available at: http://dx.doi.org/10.1029/JB091iB09p09569.

Dunlop, D. J. & Özdemir, Ö. 1997. *Rock Magnetism: Fundamentals and Frontiers*. Cambridge, UK & New York: Cambridge University Press. 573 pp.

Feely, M., Selby, D., Conliffe, J. & Judge, M. 2007. Re–Os geochronology and fluid inclusion microthermometry of molybdenite mineralisation in the late-Caledonian Omey Granite, western Ireland. *Applied Earth Science* **116**(3), 143–49.

Ferré, E. C. 2002. Theoretical models of intermediate and inverse AMS fabrics. *Geophysical Research Letters* **29**(7), 1127. Available at: http://dx.doi.org/10.1029/2001GL014367.

Gaillot, P., de Saint-Blanquat, M. & Bouchez, J.-L. 2006. Effects of magnetic interactions in anisotropy of magnetic susceptibility: Models, experiments and implications for igneous rock fabrics quantification. *Tectonophysics* **418**(1-2), 3–19.

Heider, F., Dunlop, D. J. & Soffel, H. C. 1992. Low-Temperature and Alternating Field Demagnetization of Saturation Remanence and Thermoremanence in Magnetite Grains (0.037mm to 5 mm). *Journal of Geophysical Research* **97**(B6), 9371–81.

Hopkinson, J. 1890. Magnetic Properties of Alloys of Nickel and Iron. *Proceedings of the Royal Society, London* **48**, 1–13.

Jackson, M. 1991. Anisotropy of magnetic remanence: A brief review of mineralogical sources, physical origins, and geological applications, and comparison with susceptibility anisotropy. *Pure and Applied Geophysics* **136**(1), 1–28. Available at: http://dx.doi.org/10.1007/BF00878885.

Jelinek, V. 1977. The Statistical Theory of Measuring Anisotropy of Magnetic Susceptibility of Rocks and its Application. *Geofyzika Brno* **1**, 1–88.

Jelinek, V. 1981. Characterization of the magnetic fabric of rocks. *Tectonophysics* **79**(3–4), T63–T67. Available at: http://dx.doi.org/10.1016/0040-1951(81)90110-4.

Khan, M. A. 1962. The Anisotropy of Magnetic Susceptibility of Some Igneous and Metamorphic Rocks. *Journal of Geophysical Research* **67**(7), 2873–85. Available at: http://dx.doi.org/10.1029/JZ067i007p02873.

Knight, M. D. & Walker, G. P. L. 1988. Magma flow directions in dikes of the Koolau Complex, Oahu, determined from magnetic fabric studies. *Journal of Geophysical Research: Solid Earth* **93**(B5), 4301–19. Available at: http://dx.doi.org/10.1029/JB093iB05p04301.

Lattard, D., Engelmann, R., Kontny, A. & Sauerzapf, U. 2006. Curie temperatures of synthetic titanomagnetites in the Fe–Ti–O system: Effects of composition, crystal chemistry, and thermomagnetic methods. *Journal of Geophysical Research* **111**, B12S28.

Launeau, P. & Cruden, A. R. 1998. Magmatic fabric acquisition mechanisms in a syenite: Results of a combined anisotropy of magnetic susceptibility and image analysis study. *Journal of Geophysical Research* **103**(B3), 5067–89. Available at: http://dx.doi.org/10.1029/97JB02670.

Liss, D., Owens, W. H. & Hutton, D. H. W. 2004. New palaeomagnetic results from the Whin Sill complex: evidence for a multiple intrusion event and revised virtual geomagnetic poles for the late Carboniferous for the British Isles. *Journal of the Geological Society, London* **161**(6), 927–38. Available at: http://jgs.lyellcollection.org/content/161/6/927.abstract.

Lowrie, W. & Fuller, M. 1971. On the Alternating Field Demagnetization Characteristics of Multidomain Thermoremanent Magnetization in Magnetite. *Journal of Geophysical Research* **76**(26), 6339–49.

Nagata, T. 1961. *Rock Magnetism*. Tokyo: Maruzen. 350 pp.

Orlický, O. 1990. Detection of magnetic carriers in rocks: results of susceptibility changes in powdered rock samples induced by temperature. *Physics of the Earth and Planetary Interiors* **63**, 66–70.

Owens, W. H. 1974. Mathematical model studies on factors affecting the magnetic anisotropy of deformed rocks. *Tectonophysics* **24**(1–2), 115–31. Available at: http://www.sciencedirect.com/science/article/pii/0040195174901334.

Owens, W. H. 2000. Statistical analysis of normalized and unnormalized second rank tensor data, with application to measurements of anisotropy of magnetic susceptibility. *Geophysical Research Letters* **27**(18), 2985–88. Available at: http://dx.doi.org/10.1029/1999GL008439.

Pierre, R. & Rochette, P. 1987. Magnetic susceptibility of the rock matrix related to magnetic fabric studies. *Journal of Structural Geology* **9**(8), 1015–20. Available at: http://www.sciencedirect.com/science/article/pii/0191814187900095.

Potter, D. K. & Stephenson, A. 1988. Single domain particles in rocks and magnetic fabric analysis. *Geophysical Research Letters* **15**(10), 1097–1100. Available at: http://dx.doi.org/10.1029/GL015i010p01097.

Readman, P. W. & O'Reilly, W. 1972. Magnetic properties of oxidized (cation-deficient) titanomagnetites. *Journal of Geomagnetism and Geoelectricity* **24**(1), 69–90.

Rochette, P. 1988. Inverse magnetic fabric in carbonate-bearing rocks. *Earth and Planetary Science Letters* **90**(2), 229–37. Available at: http://www.sciencedirect.com/science/article/pii/0012821X88901033.

Rochette, P., Aubourg, C. & Perrin, M. 1999. Is this magnetic fabric normal? A review and case studies in volcanic formations. *Tectonophysics* **307**(1–2), 219–34. Available at: http://www.sciencedirect.com/science/article/pii/S0040195199001274.

Rochette, P. & Vialon, P. 1984. Development of planar and linear fabrics in Dauphinois shales and slates (French Alps) studied by magnetic anisotropy and its mineralogical control. *Journal of Structural Geology* **6**(1–2), 33–38. Available at: http://www.sciencedirect.com/science/article/pii/0191814184900816.

Tarling, D. H. & Hrouda, F. (eds) 1993. *The Magnetic Anisotropy of Rocks*. London: Chapman & Hall. 217 pp.

Tauxe, L. 1998. *Paleomagnetic principles and practice*. Dordrecht, Boston: Kluwer Academic Publishers. 299 pp.

Townend, R. 1966. The geology of some granite plutons from western Connemara, Co. Galway. *Proceedings of the Royal Irish Academy*, **65 Section**(4), 157–202.

Wolff, J. A., Ellwood, B. B. & Sachs, S. D. 1989. Anisotropy of magnetic susceptibility in welded tuffs: application to a welded-tuff dyke in the tertiary Trans-Pecos Texas volcanic province, USA. *Bulletin of Volcanology* **51**(4), 299–310. Available at: http://dx.doi.org/10.1007/BF01073518.

Xu, S. & Dunlop, D. J. 1995. Toward a better understanding of the Lowrie-Fuller test. *Journal of Geophysical Research* **100**(B11), 22533–42. Available at: http://dx.doi.org/10.1029/95JB02154.